Published in final edited form as:
Immunity. 2013 February 21; 38(2): . doi:10.1016/j.immuni.2012.10.022.

Polyphasic innate immune responses to acute and chronic LCMV infection:

Innate immunity to acute & chronic viral infection

Brian A. Norris[1,2,3], **Luke S. Uebelhoer**[1,2,3], **Helder I. Nakaya**[1,2,3], **Aryn A. Price**[1,2,3], **Arash Grakoui**[1,2,3], and **Bali Pulendran**[1,2,3,*]

[1]Vaccine Research Center, Emory University, Atlanta, GA 30329

[2]Yerkes Regional Primate Research Center, Emory University, Atlanta, GA 30329

[3]Department of Pathology and Laboratory Medicine, Emory University, Atlanta, GA 30322

Summary

Resolution of acute and chronic viral infections requires activation of innate cells to initiate and maintain adaptive immune responses. Here we report that infection with acute Armstrong (ARM) or chronic Clone 13 (C13) strains of lymphocytic choriomeningitis virus (LCMV) led to two distinct phases of innate immune response. During the first 72hr of infection, dendritic cells upregulated activation markers, and stimulated anti-viral $CD8^+$ T cells, independent of viral strain. Seven days after infection, there was an increase in $Ly6C^{hi}$ monocytic and $Gr\text{-}1^{hi}$ neutrophilic cells in lymphoid organs and blood. This expansion in cell numbers was enhanced and sustained in C13 infection, whereas it occurred only transiently with ARM infection. These cells resembled myeloid-derived suppressor cells, and potently suppressed T cell proliferation. The reduction of monocytic cells in $Ccr2^{-/-}$ mice or after Gr-1 antibody depletion enhanced anti-viral T cell function. Thus, innate cells have an important immunomodulatory role throughout chronic infection.

Introduction

A fundamental feature of chronic viral infections, such as during HIV or HCV infection, is the generalized suppression of the host immune response. Innate immune responses to viral infections are essential for initiating the adaptive immune responses required for the resolution of infection and generation of long lasting immunity. Some viral infections fail to elicit sufficient immune responses or subvert host defenses, thus allowing their spread and eventual persistence. The ARM and C13 strains of LCMV have been studied for decades as models for acute and chronic infections, respectively (Ahmed et al., 1984). These strains are very closely related genetically, but the ARM strain leads to a strong $CD8^+$ T cell response that rapidly clears the virus and provides long lasting immunity (Butz and Bevan, 1998; Wherry et al., 2003b). Conversely, infection with the C13 strain of LCMV impairs virus-specific T cells, diminishing their function and enabling the persistence of the virus (Wherry

*Address correspondence and reprint requests to Dr. Bali Pulendran, Vaccine Research Center, Emory University, 954 Gatewood Road, Atlanta, GA 30329, bpulend@emory.edu.

et al., 2003a). Infection with C13 also leads to the suppression of additional immune responses to viral infections (Borrow et al., 1995; Sevilla et al., 2000).

The genome of C13 differs from ARM by two coding mutations, one in the glycoprotein (GP) and one in the polymerase protein L (Ahmed et al., 1988; Matloubian et al., 1993). The GP mutation enhances the affinity of this protein for the cellular receptor, α-dystroglycan (αDG), leading to greater infection of αDG expressing cells such as macrophages, dendritic cells (DCs) and fibroblastic reticular cells (FRC) (Matloubian et al., 1993; Mueller et al., 2007; Smelt et al., 2001). The mutation in the L protein correlates with higher levels of viral replication in plasmacytoid DCs (pDCs) and increased early viremia (Bergthaler et al., 2010). These mutations as well as similar mutations in related LCMV strains have been implicated as causing the persistence of chronic LCMV strains.

Acute LCMV infection rapidly induces DCs to upregulate the expression of costimulatory markers and gain T cell stimulatory capacity in a largely type I interferon (IFN-I) dependent manner (Montoya et al., 2005). LCMV-specific T cell responses are also highly dependent on IFN-I with maximal $CD8^+$ T cell proliferation requiring IFN-I signaling (Thompson et al., 2006). However, LCMV nucleoprotein (NP) inhibits IFN-I production in infected cells and persistent LCMV infection inhibits IFN-I production by pDCs (Martinez-Sobrido et al., 2006; Zuniga et al., 2008). IFN-I-induced STAT2 signaling inhibits the development and proliferation of DCs (Hahm et al., 2005; Sevilla et al., 2004). PD-1-PD-L1 signaling, IL-10 and TGF-β are additional immune regulatory mechanisms linked to the persistence of C13 infection and the exhaustion of the $CD8^+$ T cell response (Barber et al., 2006; Brooks et al., 2006; Tinoco et al., 2009). Despite these advances, the innate immune events that occur during the very earliest hours of infection with LCMV ARM or C13 have not been studied. Furthermore, although there have been reported defects in antigen presenting cell (APC) function during the chronic stages of C13 infection, whether such defects precede and cause dysfunctional T cell responses, and enable persistence is unclear.

We hypothesized that ARM or C13 induce distinct types of innate immune responses within the first few hours of infection, which result in the differential induction of T cell immunity and viral persistence. To address this issue, we undertook a detailed characterization of the kinetics of the innate immune responses to chronic and acute LCMV infection with a view to identifying early correlates and mechanisms of adaptive immune exhaustion and viral persistence. Two temporally distinct phases of innate immune response were observed: an early DC response during the first 72hr of infection and a later myeloid cell proliferation peaking at day 14 post infection (p.i.). We found the innate response within the first 72hr, as assessed by the numbers and activation status of DC and APC subsets and cytokine production, was largely independent of the strain of LCMV. Later during infection, as $CD8^+$ T cell responses begin to peak, there was a large expansion of myeloid cell numbers. This expansion was identical between acute and chronic strains of LCMV until about day 7. After this period, there was a rapid decline in the numbers of myeloid cells in ARM infected mice. During C13 infection, however, there was a sustained expansion of myeloid cells that exhibited the phenotype and suppressive function of myeloid-derived suppressor cells (MDSCs). Diminished recruitment of these cells or the elimination of these cells during chronic infection by depleting antibody enhanced the function of exhausted T cells. Our findings demonstrate different phases of innate cell function during viral infection and highlight an important role for innate cell inhibition of adaptive immune responses during chronic infection.

Results

Innate cell activation during first 72hr is strain independent

The innate immune responses during the first few hours of acute and chronic LCMV infection remain to be described. To address this we performed a detailed kinetic analysis of the various sub-populations of APCs, as well as induction of innate immune cytokines, within the first 72hr of infection. We directly compared innate activation to infection outcome following ARM and C13 intravenous infection at 2×10^6 p.f.u. Utilizing an 11-parameter flow cytometry panel, we identified multiple innate cell populations and gauged their activation by expression of costimulatory and inhibitory markers.

After gating on live, singlet-discriminated cells we then identified lymphocytes by expression of NK1.1, CD19, B220, and Thy1.2 (Figure S1A). In accord with previous reports (Montoya et al., 2005), there was a trend for the cellularity of LCMV infected spleens to decrease during the first 3 days of infection with both LCMV strains (Figure S1B). There was also a trend for the numbers of B, $CD4^+$ and $CD8^+$ T cells to decrease during the first 72hr.

Having removed the lymphocyte lineage from our gating we characterized the various DC populations (Figure S1C-D). pDCs can produce high amounts of IFN-I in response to viral infections or exposure to foreign nucleic acids (Diebold et al., 2003; Jung et al., 2008) and during the first few days of LCMV infection pDCs produce prodigious amounts of IFN-α (Zuniga et al., 2008). In mice, pDC can be identified as $CD11c^{lo}$, $B220^+$, $Ly6C^+$ and $CD11b^-$ (Asselin-Paturel et al., 2001) (Figure S1C). We observed a reduction in pDCs between 12-25hr post LCMV infection but pDC numbers typically rebounded around 42hr p.i. (Figure S1E). There was no difference in pDC numbers between ARM and C13 infection.

The two major murine splenic conventional DC (cDC) populations, $CD8^-$ and $CD8^+$, were identified from total non-lymphocytes by high expression of CD11c and lack of Ly6C (Figure S1D). $CD8^-$ DCs were reduced to about ¼ their initial number during the first 72hr of infection (Figure S2C). $CD8^+$ DCs cross present antigens phagocytosed from the environment via MHC Class I, and are potent initiators of Th1 cell responses (den Haan et al., 2000; Pulendran et al., 1999). In the spleen, LCMV infection leads to a substantial reduction in the numbers of these cells by day 3 of infection with either strain (Figure S2C).

Total myeloid cells were identified as $CD11c^{lo/-}$ and $CD11b^+$ and were sub-divided into three main populations; Gr-1^{lo} $Ly6C^{lo}$ $F4/80^+$ SSC^{hi} eosinophils, Gr-1^{lo} $Ly6C^{hi}$ $F4/80^+$ SSC^{lo} monocytic and Gr-1^{hi} $Ly6C^{int}$ $F4/80^-$ SSC^{int} neutrophilic cells (Figure S1F). Over the first two days, there was a trend for eosinophil, monocytic and neutrophilic cell numbers to be lower during the first 24-48hr of infection before rebounding by day 3 (Figure S1H).

We then determined the activation status of the DC subsets. cDCs expressed higher levels of CD80, CD86 and MHC Class II molecule I-A^b 25hr p.i. compared to pDCs (Figure 1A). $CD8^+$ DCs and $CD8^-$ DCs were both robustly activated, and expressed high CD80 and I-A^b. However, activation was transient and substantially reduced by day 3. In contrast, pDCs did not upregulate CD80, or I-A^b, and expression of CD86 was less than that of cDC expression. Amongst the major myeloid cell populations, only the monocytic cells showed any appreciable expression of the costimulatory marker CD86 (data not shown). Activation marker expression on all cell types was independent of the viral strain.

Furthermore, the inhibitory receptors PD-L1 and PD-L2 (Barber et al., 2006; Chen, 2004; Sharpe and Freeman, 2002) were also induced by infection. PD-L1 expression was increased

on most cell types examined following LCMV infection. The kinetics of PD-L1 upregulation was indistinguishable between ARM and C13. The expression of PD-L2 was restricted to $CD8^+$ DCs, but was only present at very low levels on these cells.

Using intracellular cytokine staining, IL-12p40 and TNF were readily detectible in cDC populations over the first day of LCMV infection (Figure 1B and data not shown), consistent with previous studies (Montoya et al., 2005). DC-produced IL-12 was detectible between 12-48hr p.i., with $CD8^+$ DCs having the highest amounts of IL-12. TNF was transiently produced by $CD8^+$ DCs during infection with similar kinetics as IL-12 (data not shown). Cytokine production by cDCs was not significantly different between acute and chronic infection.

We then assessed cytokines in the serum of LCMV infected mice. Large amounts of IFN-α were readily detected in the sera, as early as 24hr, in mice infected with either ARM or C13 (Figure 1C). In contrast, IFN-γ was only detectable at 72hr (Figure 1C). Furthermore, at 25hr p.i. IFN-induced chemokines CCL2, CXCL9, and CXCL10 were readily detectable (Figure 1C). Again, induction of these innate cytokines and chemokines was nearly identical in both ARM and C13 infection. Thus, these results indicate, as assessed by the aforementioned parameters, that innate responses to LCMV infection during the first 72hr were independent of viral strain.

Myeloid cells from C13 infected mice show impaired $CD8^+$ T cell priming

Next, we determined the stimulatory capacity of APCs from LCMV infected spleens. $CD11c^+$ DC and $CD11c^-$ $CD11b^+$ myeloid cells isolated from the spleens 24 or 48hr p.i. were cultured with OVA-specific $CD8^+$ cells from OT-I mice and SIINFEKL peptide for 3 days. Both populations stimulated T cell proliferation with as little as 0.5 pg/mL peptide (Figure 2A and data not shown). DCs were more potent stimulators than myeloid cells and were capable of inducing similar T cell proliferation with 1/10 the number of APCs. Importantly, APCs from ARM and C13 infection demonstrated nearly identical stimulatory ability.

DCs and myeloid cells from day 7 p.i. induced equivalent T cell proliferation, regardless of LCMV strain (Figure 2B). Unexpectedly, at day 14 p.i., whereas DCs from all groups were fully capable of stimulating T cells, myeloid cells from C13 infection were unable to effectively stimulate T cell proliferation. In fact, virtually no $CD8^+$ T cells seemed to survive culture, regardless of the concentration of antigenic peptide used. In contrast, myeloid cells from ARM infected spleens induced slightly lower proliferation than myeloid cells from uninfected mice, although this was evident in only in some of the experiments (Figure 2C). This deficit in proliferation was overcome by adding higher concentrations of peptide.

We measured the viral loads in $CD11c^+$ and $CD11c^-$ $CD11b^+$ populations day 14 post C13 infection to determine whether the reduced immune stimulatory capacity of the myeloid cells was a consequence of enhanced viral loads in these cells compared to DCs. We found that both populations contained measurable infectious virus, though DCs contained roughly 20× more virus than an equivalent number of myeloid cells from day 14 p.i. with C13 (data not shown). Thus, despite both DCs and myeloid cells containing virus during chronic infection, only myeloid cells lose their ability to stimulate T cells.

Chronic LCMV infection induces enhanced and sustained myeloid cell expansion

To better understand the impaired stimulatory capacity of the $CD11c^-$ $CD11b^+$ myeloid cell population during C13 infection, we determined the cellular composition of this population during infection. At day 7 p.i., when the ARM and C13 derived myeloid cells were equally

stimulatory (Figure 2), the composition of the myeloid cells was virtually identical between infections (Figure S2A). However, at day 14 p.i. the ratio of eosinophils to monocytic cells was substantially greater in ARM infected mice relative to myeloid cells from C13 infected mice (Figure S2B). The weakly stimulatory myeloid cell population isolated at day 14 during C13 infection consisted almost entirely of monocytic and neutrophilic cells.

We then evaluated myeloid cell populations over ~3 weeks of infection. Total splenic $CD11b^+$ myeloid cells, defined as described in Figure S1, increased during ARM and C13 infection between day 3-7, reaching about a 4 fold expansion above what was observed in uninfected mice (Figure 3A). Myeloid cell numbers in ARM infected mice began contracting around day 10, reaching baseline numbers by day 21. In contrast, these cells continued to increase with C13 infection, peaking between day 14 and 21 with nearly 10 fold more myeloid cells than in naïve mice (Figure 3A).

Both monocytic and neutrophilic myeloid cell populations were expanded during ARM and C13 infection (defined in Figure S1). Monocytic cell expansion peaked between days 5-7 in the spleen and blood (Figure 3B and data not shown). After day 10 of ARM infection the monocytic cells began contracting, reaching naïve levels by day 14. C13 infection led to sustained numbers of monocytic cells (about 10-fold higher than naive mice), which persisted for up to 3 weeks. Neutrophilic cells also peaked in the spleen and blood day 7 p.i. before contracting in ARM infected animals (Figure 3B and data not shown). In contrast, neutrophilic cells continued to increase during C13 infection reaching numbers more than 20 fold above naïve levels before contracting.

On day 14 p.i. the number of both monocytic and neutrophilic cells were significantly higher in the spleen, blood, and peripheral lymph nodes (pLN) of C13 infected mice compared to naïve or ARM infected mice (Figure 3C and data not shown). Histology of spleens from the peak of myeloid cell expansion during C13 infection shows a higher proportion of $F4/80^+$ myeloid cells and a corresponding loss of lymphoid-follicle structure consistent with previous reports (Figure 3D) (Odermatt et al., 1991).

Monocytic cells expanded during C13 infection resemble MDSCs

The expression of phenotypic and activation markers on myeloid cells was examined during C13 and ARM infections. Spleen monocytic cells did not show differences in expression of CD86 and $I\text{-}A^b$, however, PD-L1 expression remained elevated in C13 infected mice whilst subsiding during ARM infection. CD80 expression was also elevated on monocytic cells in lymphoid tissues and in the blood at the peak of the myeloid cell expansion during chronic infection (Figure 4A-B).. In addition, the CSF-R (CD115), which has been shown to be expressed on MDSCs in tumor models (Huang et al., 2006; Yang et al., 2006), was expressed on the monocytic cells in C13 infected mice (Figure 4C). Neutrophilic cells increased expression of PD-L1 but not CD80, CD86, $I\text{-}A^b$, or CD115 during ARM or C13 infection (data not shown).

Sorted monocytic cells from day 14 post C13 infection were very similar in morphology to naïve sorted monocytes (Figure 4D). Neutrophilic cells from day 14 C13 infected spleens showed less lobation and were predominantly in band form, representing a less mature state and further suggesting that these cells are immature myeloid cells (Figure 4D).

We then performed microarray gene expression analysis on monocytic cells sorted from naïve and day 14 ARM or C13 infected spleens to obtain insights into the regulatory networks that control the functions of these cells. Monocytic cells from C13 infected mice expressed many genes, such as *Trem1, Cd33, Ly6c1, Ptgs1, Ptgse* and *Sell* (encoding CD62L), which are known to be associated with MDSCs (Gabrilovich and Nagaraj, 2009)

(Figure 4E). In addition, there was increased expression of *Cd274* (PD-L1), *Kit*, *S100a8*, *S100a9*, and *Birc5* during both LCMV infections.

We then sought to profile the expression of genes that would give insight to the function of monocytic cells during C13 infection. Transcripts for inflammatory chemokines CXCL9 and CXCL10 were increased during both ARM and C13 infection but increases in CCL2, IL-7, CSF-1, and IL-27 cytokine transcripts above naïve levels were unique to C13 infection (Figure 4E). ARM and C13 infection also increased expression of genes that encode CCR5, IL-1R2, IL-28R, and IL-18R and decreased CX_3 CR1, IL-6, IL-10, CSF-1 and VEGF receptor transcription in monocytic cells. Only C13 infection increased transcripts for the receptors for IL-8, IL-15, IL-12, IL-20 and GM-CSF. Monocytic cells during C13 infection showed differential expression of activation induced markers, myeloid-macrophage markers, homing and recruitment genes and functional markers.

Infection with either ARM or C13 induced expression of genes related to IFN responses. Induction of 2′-5′ oligoadenylate synthetase anti-viral genes and many other IFN stimulated genes were not unique to C13 infection, however there were more of these types of genes upregulated during chronic infection. Monocytic cells also upregulated several genes related to extracellular matrix breakdown and remodeling such as matrix metallopeptidases, cathepsins and lamin. These cells also showed differential expression of approximately 80 genes related to the mitochondrial respiratory burst, including genes involved in the regulation of oxidative stress, both in genes whose products promote reactive oxygen species (ROS) production and those that mitigate ROS-related tissue damage. These ROS-related genes were predominantly induced during chronic infection. Increased ROS production has been shown to be one of the main identifiers of MDSCs in multiple tumor and infection models (Kusmartsev et al., 2004; Zhu et al., 2007). These data suggest that whilst monocytic cells from C13 infected mice express many genes that encode proinflammatory mediators; they also express genes that encode molecules involved in oxidative stress, which is implicated in tolerogenic responses.

Furthermore, monocytic cells showed a significant increase in molecules related to the processing and presentation of peptides on Class I MHC. Transcripts for proteosome subunits, peptide transporters and MHC Class I molecules were all increased in monocytic cells from C13 infected mice, relative to cells from naïve mice. Conversely, multiple genes related to MHC Class II antigen presentation were down regulated during C13 infection; transcripts for multiple MHC Class II, invariant peptide, and HLA-DM molecules were all decreased. In contrast, monocytic cells from acute infection increased transcription for only a few Class I genes and upregulated some Class II related genes.

Overall these data reveal a distinctive molecular signature of monocytic cells isolated from C13 infected mice, relative to those from ARM infected or naïve mice. Taken together, the phenotypic, morphological and transcriptional signatures suggest that myeloid cells from C13 infected mice resemble MDSCs.

Myeloid cells suppress T cell proliferation *ex vivo*

MDSCs expand during multiple tumor models can potently suppress T cell responses (Youn et al., 2008). The substantial increase of myeloid cells during chronic LCMV infection coincided with the functional exhaustion of LCMV-specific $CD8^+$ T cells (Figure 5A), raising the possibility that myeloid cells suppressed LCMV-specific $CD8^+$ T cells.

To determine if these cells were immunosuppressive we sort purified monocytic cells and co-cultured them with total splenocytes from OT1 mice and stimulated with SIINFEKL peptide. Monocytic cells from day 14 post-C13 infection suppressed OT-I T cell

proliferation in a cell number dependent manner (Figure 5B). Naïve and ARM derived myeloid cells had no effect on the proliferation of the T cells even at high ratios. Monocytic cells from C13 infected mice were also able to suppress T cell responses in a different system using plate bound anti-CD3 and anti-CD28 stimulation of T cells from OT-1 mice (Figure 5C-D). Interestingly, however, undivided $CD8^+$ T cells seem to survive culture, when plate bound stimulation with anti-CD3ε and anti-CD28 was used, presumably because of survival signals delivered via these receptors to T cells. Neutrophilic cells could suppress T cell responses when OT-1 cells were used in the presence of SIINFEKL peptide, but were unable to induce suppression in the system using plate bound anti-CD3 and -CD28 stimulation of T cells (data not shown).

MDSCs from tumor and other models systems have been reported to suppress T cell proliferation by metabolism of L-arginine by inducible nitric oxide synthase (iNOS) and arginase1 (ARG1). To determine the mechanism by which monocytic cells suppress T cell proliferation, these cells were cultured with $CD8^+$ T cells from OT-1 mice, with or without inhibitors against the aforementioned molecules. With the addition of the iNOS-specific inhibitor L-NIL or total NOS inhibitor L-NMMA the proliferation of T cells was restored. Additionally, blocking antibodies to IFN-γ, which is known to induce iNOS (Melillo et al., 1994), alleviated suppression. Neither the addition of ARG1 inhibitor, nor-NOHA, or blocking antibodies to IL-10R, TGF-β, or PD-1 were able to restore suppression. Monocytic MDSCs derived from chronic LCMV infection limit T cell proliferation via IFN-γ induced iNOS production of NO.

Mobilization of monocytic suppressor cells is dependent on CCR2

The two major monocytic cell subsets in mice are typically distinguished by their differential expression of chemokine receptors and other surface markers. ‘Classical’ monocytes have been described as $CCR2^+$, $Ly6C^{hi}$, CX_3CR1^+, and $CD62L^+$ while ‘non-classical’ monocytes are $CCR2^-$, $Ly6C^{Int}$, $CX3CR1^{++}$, and $CD62L^-$ (Geissmann et al., 2003). CCL2 is known to be a ligand for CCR2 and previous studies have demonstrated that the recruitment of MDSCs to tumors was mediated by CCR2-CCL2 signaling and depletion of $CCR2^+$ cells enhanced antigen specific $CD8^+$ T cell responses (Huang et al., 2007; Lesokhin et al., 2012). We therefore determined whether recruitment of MDSCs during C13 infection was dependent on CCR2.

We first measured the serum concentrations of CCL2 throughout acute and chronic LCMV infection (Figure 6A). Both ARM and C13 infection led to a high amount of CCL2 24hr p.i. (Figure 1C). CCL2 concentrations were still significantly elevated day 7 p.i. but by day 10 the chemokine concentration had dropped during ARM infection to near baseline levels. In contrast, CCL2 concentrations following C13 infection remained markedly elevated over baseline and ARM levels as late as 28 days p.i.

Upon infection of WT and $Ccr2^{-/-}$ mice with C13, we observed that $Ccr2^{-/-}$ mice showed significantly increased concentrations of CCL2 in the serum 14 days p.i. (Figure 6B). Monocytic cells expanded in the spleen, pLN, blood and liver were predominantly $CCR2^+$ at both day 7 and day 14 post C13 infection (Figure 6C and data not shown). The numbers of monocytic cells in the blood at these times were significantly lower in C13 infected $Ccr2^{-/-}$ mice than infected controls (Figure 6D), despite the elevated levels of CCL2. This is consistent with previous reports that $Ccr2^{-/-}$ monocytes are defective at migrating from the bone marrow to the blood (Serbina and Pamer, 2006). Lower numbers of monocytic cells in the blood of $Ccr2^{-/-}$ mice were evident even 14 days p.i., although the numbers of such cells in both $Ccr2^{-/-}$ and WT mice had increased relative to day 7 (Figure 6D).

In the spleen, there was a marked reduction in monocytic cell numbers in *Ccr2*$^{-/-}$ mice at day 7 p.i., although at day 14 there was equilibration of the numbers between WT and *Ccr2*$^{-/-}$ mice (Figure 6E). This suggests that while CCR2 plays a key role in the exit of monocytic cells from the bone marrow to the blood, it plays little or no role in the migration of such cells from the blood to the spleen (Serbina et al., 2008). When multiple lymphocyte and DC populations were measured day 14 p.i. we observed that T cell, pDC, and cDC numbers were equivalent in the spleen and pLN of B6 and *Ccr2*$^{-/-}$ mice (Figure S3A-B). Only B cells in the spleen of *Ccr2*$^{-/-}$ mice were slightly diminished compared to WT.

Given the reduced numbers of monocytic cells in the spleens of C13 infected *Ccr2*$^{-/-}$ mice at day 7, we assessed the magnitude of antigen-specific CD8^{+} T cell responses. Cytokine expression by CD8^{+} T cells stimulated ex vivo with three immunodominant MHC Class I peptides were not significantly different in *Ccr2*$^{-/-}$ and B6 mice day 7 p.i. (Figure 6F and Figure S3C). However, by day 14 the cytokine responses of LCMV-specific T cells were significantly elevated in frequency and absolute number in the *Ccr2*$^{-/-}$ mice (Figure S3C). Taken together, these data demonstrate a decreased mobilization of monocytic cells from the bone marrow into circulation during chronic infection of *Ccr2*$^{-/-}$ mice. This diminished pool of blood monocytic cells delays their recruitment to the spleen, thereby reducing the number of MDSCs in lymphoid tissues, and decreasing the opportunity for T cell suppression.

Antibody depletion of myeloid cells enhances LCMV-specific T cell responses *in vivo*

To test specifically whether myeloid cells during C13 infection inhibit T cell responses and contribute to T cell exhaustion we depleted total myeloid cells with an antibody against Gr-1. We treated mice with 100 μg of anti-Gr-1 for three days prior to the peak of myeloid cell expansion on day 14. It has been previously reported that anti-Gr-1 does not completely deplete Gr-1^{+} cells and leaves a population with the antibody on the surface for more than four days following treatment (Ribechini et al., 2009). Staining with a secondary antibody recognizing the depleting antibody confirmed that there was significant occlusion of the Gr-1 epitope (data not shown) that blocked fluorophore-conjugated RB6-8C5 (Ly6C/G) and 1A8 (anti-Ly6G) antibody staining. Because of this we measured total non-lymphocyte, non-DC, myeloid cells. Treatment with anti-Gr-1 significantly reduced the total numbers of myeloid cells in the spleen and blood (Figure 7A-B) to levels seen in naïve mice. On average, relative to untreated mice, antibody treated mice had 1/10 and 1/6 the number of myeloid cells in the blood and spleen, respecitively. Using expression of F4/80 by monocytic cells and DEC-205 by neutrophilic cells it was possible to subdivide the monocytic populations independent of Gr-1 expression. In the blood and spleen there was a significant reduction in monocytic cells, and in the blood, spleen and pLN there was significant reduction of neutrophilic cells (Figure S4A-B).

The depletion was specific to myeloid cells with there being no significant reduction in total lymphocyte and DC numbers in the spleen or pLN (Figure S4C-D). The depletion of myeloid cells correlated with a significant increase in the frequency of virus-specific functional T cell responses. Depleted mice showed increased frequencies and absolute numbers of IFN-γ, TNF, and IL-2 producing LCMV-specific T cells in the spleen (Figure 7C and Figure S4E). These cells were also more polyfunctional than T cells from untreated mice, having increased proportions of IFN-γ and TNF double positive cells (data not shown). Myeloid cells were also reduced by half in the pLN (Figure 7D) and had a corresponding increase in CD8^{+} T cell function (Figure 7E and Figure SF). There was trend for viral loads to be reduced following depletion of myeloid cells, although this was not statistically significant (data not shown). Our data suggests that by reducing the numbers of suppressive myeloid cells we were able to boost CD8^{+} T cell function.

Discussion

Diminished $CD8^+$ T cell number and function has been attributed to the persistence of viral infections in both humans and mice (Klenerman and Hill, 2005; Zajac et al., 1998). In this study we show that during the T cell priming phase of LCMV infection both ARM and C13 strains activate innate APCs and induce phenotypic and functional changes with virtually identical kinetics. Following the induction of T cell responses, C13 infection leads to a massive expansion and accumulation of myeloid cells with T cell suppressive function.

Persistently infecting strains of LCMV initially infect marginal zones by 24hr p.i., then progress to the interdigitating DC of the white pulp by day 3 p.i. In contrast, acutely infecting strains are restricted to the red pulp of the spleen (Borrow et al., 1995; Smelt et al., 2001). This difference in tropism has been attributed to the higher affinity of the viral GP for its cellular receptor, αDG, which is highly expressed on DCs, and results in a much higher viral burden in splenic DCs (Sevilla et al., 2000). Our data suggests that despite these differences, during the first three days of infection persistent and chronic strains of LCMV similarly affect the activation and function of innate APCs. The upregulation of activation markers and pro-inflammatory cytokines by DC and myeloid populations during the first three days is independent of viral strain.

Both DC and myeloid cells are capable of stimulating T cell proliferation and differentiation during the first few days of infection with acute or chronic LCMV. Addition of exogenous peptide to APC cultures leads to nearly identical proliferation T cells. It is important to note that these data do not preclude the possibility that APCs during acute or chronic infection have different antigen loads or specific impairments in presenting viral antigens on MHC molecules.

Although we could not demonstrate any functional deficit in DC purified from acute or chronically infected mice, we observed that $CD11b^+$ myeloid cells from chronically infected mice 14 days p.i. were not only unable to stimulate T cells, but they actively suppressed the priming of T cells. Both the monocytic and neutrophilic cells, profoundly expanded during C13 infection, had the appearance of MDSCs as described in multiple models of chronic infection (Gallina et al., 2006; Voisin et al., 2004; Zhu et al., 2007).

It is important to emphasize that while myeloid cells are expanded during day 7 post both ARM and C13 infection, these cells were not observed to be suppressive at this time. Only after this point to do we observe suppression of T cell proliferation by C13 derived $CD11c^-$ $CD11b^+$ myeloid cells. We cannot formally exclude the possibility that early on both infections induce some suppressive activities in myeloid cells, but C13 infection clearly leads to the sustained and enhanced suppressive function of these cells.

Although CCR2 is important to the egress of monocytes from the bone marrow into the blood, the entry of monocytes into inflamed tissues is not CCR2-dependent and can happen by a variety of other receptors, including CCR5 (Serbina and Pamer, 2006). Indeed, our gene chip data suggests that CCR5 is upregulated on monocytic cells during infection and may be an alternative mechanism for MDSC accumulation in tissues. The diminished level of circulating monocytic cells and alternative egress mechanisms may cause $Ccr2^{-/-}$ MDSC entry into the spleen with slightly delayed kinetics, delaying their suppressive effect on T cells.

Currently there are no known markers specific to murine MDSC. We have used an antibody recognizing one of the predominant markers expressed by MDSC, Gr-1, to deplete myeloid cells expanded during C13 infection. The RB6-8C5 antibody clone has been used for years to deplete neutrophils, monocytes and MDSC in a variety of settings (Daley et al., 2008;

Delano et al., 2007; Kim et al., 2009). We used a dose and regimen of antibody delivery that reduced both neutrophilic and monocytic cell populations in the blood, spleen and pLN, while not significantly decreasing other cell types. The loss of myeloid cells correlated with enhanced $CD8^+$ T cell function, but surprisingly did not significantly impact viral loads. The failure eliminate virus may be due to multiple factors. Although myeloid cells are infected by C13, they are but one of many cell types, including DCs and FRCs, which are highly infected by C13. Thus it was not surprising that the depletion of myeloid cells did not in itself lower viral loads. We administered antibody during the window when myeloid cells began to diverge in ARM and C13 infection, for only 3 days. This is likely insufficient time for the $CD8^+$ T cells to significantly impact viral loads and eliminate the signals leading to further MDSC expansion and function. Additionally, RB6-8C5 can also transmit signals via STAT1, STAT3 and STAT5 and consequently induce BM myelopoeisis, induce apoptosis in granulocytes and cause transient loss of MDSC suppressive function (Ribechini et al., 2009). These factors which complicate the use of this antibody as a treatment for chronic LCMV infection. Furthermore, MDSC may be just one of several factors (e.g. PD1-PDL1, IL-10, and TGF-β) involved in the suppression of T cell responses and persistence of viral infection during C13 infection.

It seems that there is no inherent defect in the initial priming of $CD8^+$ T cells during chronic LCMV infection compared to acute infection. However, the increased infectivity of DC, myeloid cells and FRC by persistent strains of LCMV and their faster replication likely outpaces the ability of the innate and adaptive immune responses to contain the infection. In addition to increasing the opportunity for T cells to receive antigenic stimulation which drives T cell exhaustion (Mueller and Ahmed, 2009), widespread C13 infection increases the number and dissemination of infected targets for CTL killing. CTL lysis of infected cells is the cause of immunopathology during C13 infection and can risk the survival of the infected animal. Following the loss of infected accessory and hematopoietic cells to CTL killing, and in response to stimulatory signals such as CCL2, myeloid progenitor cells are mobilized from the bone marrow to replace the dead cells. Upon entering tissues experiencing prolonged inflammation, with both innate and adaptive effector cytokines present, myeloid precursors gain a suppressive function. IFN-γ produced upon recognition of viral antigens can induce iNOS production in monocytic cells, and in turn inhibit T cell function. MDSCs, in concert with multiple suppressive mechanisms counter the excessive activation of the innate immune system and immunopathology caused by the persistence of pathogens during chronic infections (Medzhitov et al., 2012), but consequently hinder viral clearance.

The appearance of large numbers of MDSCs during chronic inflammation appears to be a common feedback mechanism in both mice and humans. Because of this, many different avenues of combating MDSC number, function and generation are being actively pursued (Gabrilovich and Nagaraj, 2009). Having implicated MDSCs in the suppression of T cell responses during LCMV infection, and demonstrating that depletion of these cells can enhance T cell function, we believe that counteracting MDSC effects is likely to be an important additional way to confront difficulties in treating chronic human infections like HIV and HCV. Taken together, the data presented in this study highlight the polyphasic nature of the innate responses to viral infections, and reveal a continuing role for the innate immune system throughout the course of persistent viral infections.

Experimental Procedures

Mice and Viruses

C57BL/6 (Charles River Laboratory), OT-I(Rag1/2$^{+/+}$) and *Ccr2*$^{-/-}$ B6.129S4-Ccr^{tm1Ifc}/J (The Jackson Laboratory), B6.129S7-*Rag1*^{tm1Mom} Tg(TcraTcrb)1100Mjb N9+N1(OT-

I($Rag1^{-/-}$)(Taconic) mice were maintained under specific pathogen-free conditions in the Emory Vaccine Center vivarium. All of the animal protocols were reviewed and approved by the Institute Animal Care and Use Committee of Emory University. LCMV strains ARM and C13 from Rafi Ahmed and Joshy Jacob (Emory Vaccine Center, Emory University, Atlanta, GA) were grown and quantified as described (Ahmed et al., 1984; Borrow et al., 1995).

Flow Cytometry

Spleens from naïve and LCMV infected mice were collagenase digested as described (Dillon et al., 2006). Collagenase digested splenocytes were stained with multiple mAb and samples were acquired on a BD Biosciences LSR II and analyzed using FlowJo (TreeStar, Inc). Geometric mean fluorescence intensities of activation markers were normalized to non-specific isotype controls. The normalization was calculated as $(gMFI_{marker} - gMFI_{isotype}) / gMFI_{isotype}$. Further details are in supplementary data.

Serum Cytokine Analysis

Serum pooled from three mice was assayed with Bio Rad and Invitrogen multi-cytokine detection panels. Data were acquired using the Luminex 100 reader and analyzed with Masterplex Quantitation software (Miraibio). ELISAs were performed for of IFN-γ (eBioscience), IFN-α (PBL InterferonSource), and CCL2 (R&D Systems).

APC Functional Assays

Total DC and myeloid cells were purified from the collagenase digested spleens of infected mice 24hr, days 7 and day 14 p.i. Splenocytes were depleted with anti-CD19 coated microbeads (Miltenyi) then positively selected by anti-$CD11c^+$ microbeads. Total myeloid cells were purified from the $CD11c^-$ fraction by using anti-$CD11b^+$ microbeads. Total DC and myeloid cell populations were determined as >95% pure by flow cytometry.

Purified DC or myeloid cells were cultured with 10^5 CFSE-labeled $CD8^+$ OT-I T cells at a ratio of 1:10 or 1:1 respectfully. Cells were cultured with SIINFEKL peptide (a generous gift from Dr. Jan Pohl, Biotechnology Branch, CDC, Atlanta, GA) for three days before being stained with anti-CD8 and anti-Thy1.2 (BD Pharmingen) and analyzed on an LSR II flow cytometer.

T Cell Suppression Assay

Total $CD11b^+$ cells enriched from the spleens of 5 naïve or day 14 LCMV infected mice using MACS beads before being sorted on a FACS Aria II (BD Biosciences) into $Ly6C^{hi}$, $Gr\text{-}1^{int}$ and $Ly6C^{int}$, $Gr\text{-}1^{hi}$ populations. The average purity of monocytic cell populations from 3 experiments was >93%. Myeloid cells were added to 10^5 OTI responder splenocytes and cultured for 24h with SIINFEKL or control Vaccinia peptide (B8R) before [^{3}H]thymidine was added and proliferation was evaluated as previously described (Youn et al., 2008). In other assays, sort purified monocytic cells from day 14 C13 infection were cultured 1:2 with 10^5 purified and CFSE labeled $CD8^+$ cells and stimulated with plate bound anti-CD3ε and anti-CD28 for three days. Inhibitors L-NIL (0.5 mM, Sigma-Aldrich), nor-NOHA (0.5 mM, Cayman Chemical Company), L-NMMA (5 mM, Calbiochem), and blocking antibodies anti-IFN-γ (XMG1.2, 10μg/mL), anti-IL-10R (1B1.3a, 20μg/mL, Biolegend), anti-PD1 (J43, 10μg/mL, eBioscience) and anti-$TGF\text{-}\beta_{1,2,3}$ (1D11, 10μg/mL, R&D Systems) were added at the beginning of culture.

Gene expression analyses

Total RNA from sorted splenic monocytic cells of naïve and day 14 C13 infected mice were purified using Trizol (Invitrogen). Relative gene expression was enumerated using Illumina MouseWG-6 v2.0 Expression BeadChips. Further details are in supplementary data.

Myeloid Cell Depletion

Mice infected with C13 were given intraperitoneal injections of 100 μg of anti-Gr-1 (RB6-8C5) (Bio X Cell) or isotype control antibody at days 11, 12 and 13 p.i. Spleens, LN, blood were collected on day 14.

Statistics

Statistical significance was determined by Mann-Whitney tests using Prism (GraphPad Software). Probability values of $p \leq 0.05$ were considered significant.

Supplementary Material

Refer to Web version on PubMed Central for supplementary material.

Acknowledgments

We gratefully acknowledge Dr. Rafi Ahmed for advice and discussion, Drs. Brian Evavold and Joshy Jacob, and Ruth Napier for comments on the paper; Barbara Cervasi and Kiran Gill for outstanding help with myeloid cell sorting; John Connolly's core laboratory at the Baylor Institute (Dallas, TX) for luminex analysis. This work was supported by grants U54AI057157, R37AI48638, R37DK057665, U19AI057266, HHSN266200700006C, NO1 AI50025 and U19AI090023 from the National Institutes of Health and a grant from the Bill & Melinda Gates Foundation. Additional support was provided by the Yerkes Research Center Base Gran RR-00165, and Public Health Service DK083356 and Al070101 (AG).

References

Ahmed R, Salmi A, Butler LD, Chiller JM, Oldstone MB. Selection of genetic variants of lymphocytic choriomeningitis virus in spleens of persistently infected mice. Role in suppression of cytotoxic T lymphocyte response and viral persistence. The Journal of experimental medicine. 1984; 160:521–540. [PubMed: 6332167]

Ahmed R, Simon RS, Matloubian M, Kolhekar SR, Southern PJ, Freedman DM. Genetic analysis of in vivo-selected viral variants causing chronic infection: importance of mutation in the L RNA segment of lymphocytic choriomeningitis virus. J Virol. 1988; 62:3301–3308. [PubMed: 3261347]

Asselin-Paturel C, Boonstra A, Dalod M, Durand I, Yessaad N, Dezutter-Dambuyant C, Vicari A, O'Garra A, Biron C, Briere F, Trinchieri G. Mouse type I IFN-producing cells are immature APCs with plasmacytoid morphology. Nature immunology. 2001; 2:1144–1150. [PubMed: 11713464]

Barber DL, Wherry EJ, Masopust D, Zhu B, Allison JP, Sharpe AH, Freeman GJ, Ahmed R. Restoring function in exhausted CD8 T cells during chronic viral infection. Nature. 2006; 439:682–687. [PubMed: 16382236]

Bergthaler A, Flatz L, Hegazy AN, Johnson S, Horvath E, Lohning M, Pinschewer DD. Viral replicative capacity is the primary determinant of lymphocytic choriomeningitis virus persistence and immunosuppression. Proc Natl Acad Sci U S A. 2010; 107:21641–21646. [PubMed: 21098292]

Borrow P, Evans CF, Oldstone MB. Virus-induced immunosuppression: immune system-mediated destruction of virus-infected dendritic cells results in generalized immune suppression. J Virol. 1995; 69:1059–1070. [PubMed: 7815484]

Brooks DG, Trifilo MJ, Edelmann KH, Teyton L, McGavern DB, Oldstone MB. Interleukin-10 determines viral clearance or persistence in vivo. Nature medicine. 2006; 12:1301–1309.

Butz EA, Bevan MJ. Massive expansion of antigen-specific CD8+ T cells during an acute virus infection. Immunity. 1998; 8:167–175. [PubMed: 9491998]

Chen L. Co-inhibitory molecules of the B7-CD28 family in the control of T-cell immunity. Nature reviews. 2004; 4:336–347.

Daley JM, Thomay AA, Connolly MD, Reichner JS, Albina JE. Use of Ly6G-specific monoclonal antibody to deplete neutrophils in mice. J Leukoc Biol. 2008; 83:64–70. [PubMed: 17884993]

Delano MJ, Scumpia PO, Weinstein JS, Coco D, Nagaraj S, Kelly-Scumpia KM, O'Malley KA, Wynn JL, Antonenko S, Al-Quran SZ, et al. MyD88-dependent expansion of an immature Gr-1(+)CD11b(+) population induces T cell suppression and Th2 polarization in sepsis. The Journal of experimental medicine. 2007; 204:1463–1474. [PubMed: 17548519]

den Haan JM, Lehar SM, Bevan MJ. CD8(+) but not CD8(−) dendritic cells cross-prime cytotoxic T cells in vivo. The Journal of experimental medicine. 2000; 192:1685–1696. [PubMed: 11120766]

Diebold SS, Montoya M, Unger H, Alexopoulou L, Roy P, Haswell LE, Al-Shamkhani A, Flavell R, Borrow P, Reis e Sousa C. Viral infection switches non-plasmacytoid dendritic cells into high interferon producers. Nature. 2003; 424:324–328. [PubMed: 12819664]

Dillon S, Agrawal S, Banerjee K, Letterio J, Denning TL, Oswald-Richter K, Kasprowicz DJ, Kellar K, Pare J, van Dyke T, et al. Yeast zymosan, a stimulus for TLR2 and dectin-1, induces regulatory antigen-presenting cells and immunological tolerance. The Journal of clinical investigation. 2006; 116:916–928. [PubMed: 16543948]

Gabrilovich DI, Nagaraj S. Myeloid-derived suppressor cells as regulators of the immune system. Nature reviews. 2009; 9:162–174.

Gallina G, Dolcetti L, Serafini P, De Santo C, Marigo I, Colombo MP, Basso G, Brombacher F, Borrello I, Zanovello P, et al. Tumors induce a subset of inflammatory monocytes with immunosuppressive activity on CD8+ T cells. The Journal of clinical investigation. 2006; 116:2777–2790. [PubMed: 17016559]

Geissmann F, Jung S, Littman DR. Blood monocytes consist of two principal subsets with distinct migratory properties. Immunity. 2003; 19:71–82. [PubMed: 12871640]

Hahm B, Trifilo MJ, Zuniga EI, Oldstone MB. Viruses evade the immune system through type I interferon-mediated STAT2-dependent, but STAT1-independent, signaling. Immunity. 2005; 22:247–257. [PubMed: 15723812]

Huang B, Lei Z, Zhao J, Gong W, Liu J, Chen Z, Liu Y, Li D, Yuan Y, Zhang GM, Feng ZH. CCL2/CCR2 pathway mediates recruitment of myeloid suppressor cells to cancers. Cancer Lett. 2007; 252:86–92. [PubMed: 17257744]

Huang B, Pan PY, Li Q, Sato AI, Levy DE, Bromberg J, Divino CM, Chen SH. Gr-1+CD115+ immature myeloid suppressor cells mediate the development of tumor-induced T regulatory cells and T-cell anergy in tumor-bearing host. Cancer Res. 2006; 66:1123–1131. [PubMed: 16424049]

Jung A, Kato H, Kumagai Y, Kumar H, Kawai T, Takeuchi O, Akira S. Lymphocytoid choriomeningitis virus activates plasmacytoid dendritic cells and induces a cytotoxic T-cell response via MyD88. J Virol. 2008; 82:196–206. [PubMed: 17942529]

Kim JV, Kang SS, Dustin ML, McGavern DB. Myelomonocytic cell recruitment causes fatal CNS vascular injury during acute viral meningitis. Nature. 2009; 457:191–195. [PubMed: 19011611]

Klenerman P, Hill A. T cells and viral persistence: lessons from diverse infections. Nature immunology. 2005; 6:873–879. [PubMed: 16116467]

Kusmartsev S, Nefedova Y, Yoder D, Gabrilovich DI. Antigen-specific inhibition of CD8+ T cell response by immature myeloid cells in cancer is mediated by reactive oxygen species. J Immunol. 2004; 172:989–999. [PubMed: 14707072]

Lesokhin AM, Hohl TM, Kitano S, Cortez C, Hirschhorn-Cymerman D, Avogadri F, Rizzuto GA, Lazarus JJ, Pamer EG, Houghton AN, et al. Monocytic CCR2(+) myeloid-derived suppressor cells promote immune escape by limiting activated CD8 T-cell infiltration into the tumor microenvironment. Cancer Res. 2012; 72:876–886. [PubMed: 22174368]

Martinez-Sobrido L, Zuniga EI, Rosario D, Garcia-Sastre A, de la Torre JC. Inhibition of the type I interferon response by the nucleoprotein of the prototypic arenavirus lymphocytic choriomeningitis virus. J Virol. 2006; 80:9192–9199. [PubMed: 16940530]

Matloubian M, Kolhekar SR, Somasundaram T, Ahmed R. Molecular determinants of macrophage tropism and viral persistence: importance of single amino acid changes in the polymerase and

glycoprotein of lymphocytic choriomeningitis virus. J Virol. 1993; 67:7340–7349. [PubMed: 7693969]

Medzhitov, R.; Schneider, DS.; Soares, MP. Science. Vol. 335. New York, N.Y: 2012. Disease tolerance as a defense strategy; p. 936-941.

Melillo G, Cox GW, Biragyn A, Sheffler LA, Varesio L. Regulation of nitric-oxide synthase mRNA expression by interferon-gamma and picolinic acid. The Journal of biological chemistry. 1994; 269:8128–8133. [PubMed: 7510678]

Montoya M, Edwards MJ, Reid DM, Borrow P. Rapid activation of spleen dendritic cell subsets following lymphocytic choriomeningitis virus infection of mice: analysis of the involvement of type 1 IFN. J Immunol. 2005; 174:1851–1861. [PubMed: 15699111]

Mueller SN, Ahmed R. High antigen levels are the cause of T cell exhaustion during chronic viral infection. Proc Natl Acad Sci U S A. 2009; 106:8623–8628. [PubMed: 19433785]

Mueller SN, Matloubian M, Clemens DM, Sharpe AH, Freeman GJ, Gangappa S, Larsen CP, Ahmed R. Viral targeting of fibroblastic reticular cells contributes to immunosuppression and persistence during chronic infection. Proc Natl Acad Sci U S A. 2007; 104:15430–15435. [PubMed: 17878315]

Odermatt B, Eppler M, Leist TP, Hengartner H, Zinkernagel RM. Virus-triggered acquired immunodeficiency by cytotoxic T-cell-dependent destruction of antigen-presenting cells and lymph follicle structure. Proc Natl Acad Sci U S A. 1991; 88:8252–8256. [PubMed: 1910175]

Pulendran B, Smith JL, Caspary G, Brasel K, Pettit D, Maraskovsky E, Maliszewski CR. Distinct dendritic cell subsets differentially regulate the class of immune response in vivo. Proc Natl Acad Sci U S A. 1999; 96:1036–1041. [PubMed: 9927689]

Ribechini E, Leenen PJ, Lutz MB. Gr-1 antibody induces STAT signaling, macrophage marker expression and abrogation of myeloid-derived suppressor cell activity in BM cells. Eur J Immunol. 2009; 39:3538–3551. [PubMed: 19830733]

Serbina NV, Jia T, Hohl TM, Pamer EG. Monocyte-mediated defense against microbial pathogens. Annual review of immunology. 2008; 26:421–452.

Serbina NV, Pamer EG. Monocyte emigration from bone marrow during bacterial infection requires signals mediated by chemokine receptor CCR2. Nature immunology. 2006; 7:311–317. [PubMed: 16462739]

Sevilla N, Kunz S, Holz A, Lewicki H, Homann D, Yamada H, Campbell KP, de La Torre JC, Oldstone MB. Immunosuppression and resultant viral persistence by specific viral targeting of dendritic cells. The Journal of experimental medicine. 2000; 192:1249–1260. [PubMed: 11067874]

Sevilla N, McGavern DB, Teng C, Kunz S, Oldstone MB. Viral targeting of hematopoietic progenitors and inhibition of DC maturation as a dual strategy for immune subversion. The Journal of clinical investigation. 2004; 113:737–745. [PubMed: 14991072]

Sharpe AH, Freeman GJ. The B7-CD28 superfamily. Nature reviews. 2002; 2:116–126.

Smelt SC, Borrow P, Kunz S, Cao W, Tishon A, Lewicki H, Campbell KP, Oldstone MB. Differences in affinity of binding of lymphocytic choriomeningitis virus strains to the cellular receptor alpha-dystroglycan correlate with viral tropism and disease kinetics. J Virol. 2001; 75:448–457. [PubMed: 11119613]

Thompson LJ, Kolumam GA, Thomas S, Murali-Krishna K. Innate inflammatory signals induced by various pathogens differentially dictate the IFN-I dependence of CD8 T cells for clonal expansion and memory formation. J Immunol. 2006; 177:1746–1754. [PubMed: 16849484]

Tinoco R, Alcalde V, Yang Y, Sauer K, Zuniga EI. Cell-intrinsic transforming growth factor-beta signaling mediates virus-specific CD8+ T cell deletion and viral persistence in vivo. Immunity. 2009; 31:145–157. [PubMed: 19604493]

Voisin MB, Buzoni-Gatel D, Bout D, Velge-Roussel F. Both expansion of regulatory GR1+ CD11b+ myeloid cells and anergy of T lymphocytes participate in hyporesponsiveness of the lung-associated immune system during acute toxoplasmosis. Infection and immunity. 2004; 72:5487–5492. [PubMed: 15322051]

Wherry EJ, Blattman JN, Murali-Krishna K, van der Most R, Ahmed R. Viral persistence alters CD8 T-cell immunodominance and tissue distribution and results in distinct stages of functional impairment. J Virol. 2003a; 77:4911–4927. [PubMed: 12663797]

Wherry EJ, Teichgraber V, Becker TC, Masopust D, Kaech SM, Antia R, von Andrian UH, Ahmed R. Lineage relationship and protective immunity of memory CD8 T cell subsets. Nature immunology. 2003b; 4:225–234. [PubMed: 12563257]

Yang R, Cai Z, Zhang Y, Yutzy WHt, Roby KF, Roden RB. CD80 in immune suppression by mouse ovarian carcinoma-associated Gr-1+CD11b+ myeloid cells. Cancer Res. 2006; 66:6807–6815. [PubMed: 16818658]

Youn JI, Nagaraj S, Collazo M, Gabrilovich DI. Subsets of myeloid-derived suppressor cells in tumor-bearing mice. J Immunol. 2008; 181:5791–5802. [PubMed: 18832739]

Zajac AJ, Blattman JN, Murali-Krishna K, Sourdive DJ, Suresh M, Altman JD, Ahmed R. Viral immune evasion due to persistence of activated T cells without effector function. The Journal of experimental medicine. 1998; 188:2205–2213. [PubMed: 9858507]

Zhu B, Bando Y, Xiao S, Yang K, Anderson AC, Kuchroo VK, Khoury SJ. CD11b+Ly-6C(hi) suppressive monocytes in experimental autoimmune encephalomyelitis. J Immunol. 2007; 179:5228–5237. [PubMed: 17911608]

Zuniga EI, Liou LY, Mack L, Mendoza M, Oldstone MB. Persistent virus infection inhibits type I interferon production by plasmacytoid dendritic cells to facilitate opportunistic infections. Cell Host Microbe. 2008; 4:374–386. [PubMed: 18854241]

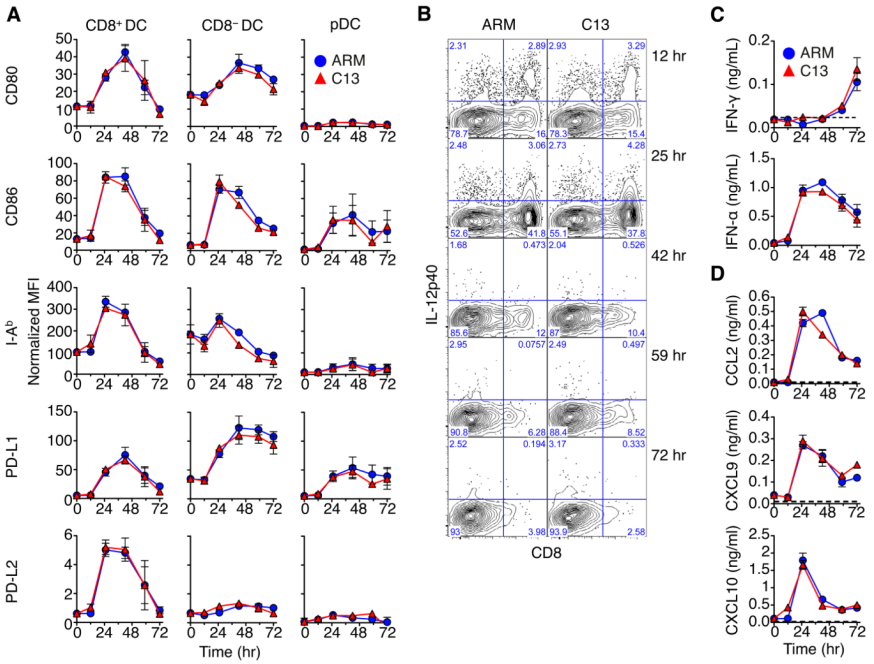

Figure 1. see also Figure S1: The kinetics of APC activation and innate cytokine production are LCMV strain independent

(A) The normalized MFI of activation markers on DC populations relative to isotype control during early LCMV infection. Data are represented as mean ± SEM of 3 experiments with 3 pooled spleens for each time point.

(B) Representative intracellular staining for IL-12p40 of splenocytes over indicated time. Numbers in the quadrant represent percent cytokine expression in cDC from LCMV infected mice.

(C) Serum IFN concentrations in naïve and LCMV infected mice as quantified by ELISA. Data are represented as mean ± SEM of 3 independent experiments with 3 mice per time point.

(D) Serum chemokine levels in naïve and LCMV infected mice as quantified by luminex bead assay. Data are represented as mean ± SEM and are representative of two independent luminex assays of serum pooled from 3 mice and analyzed in duplicate.

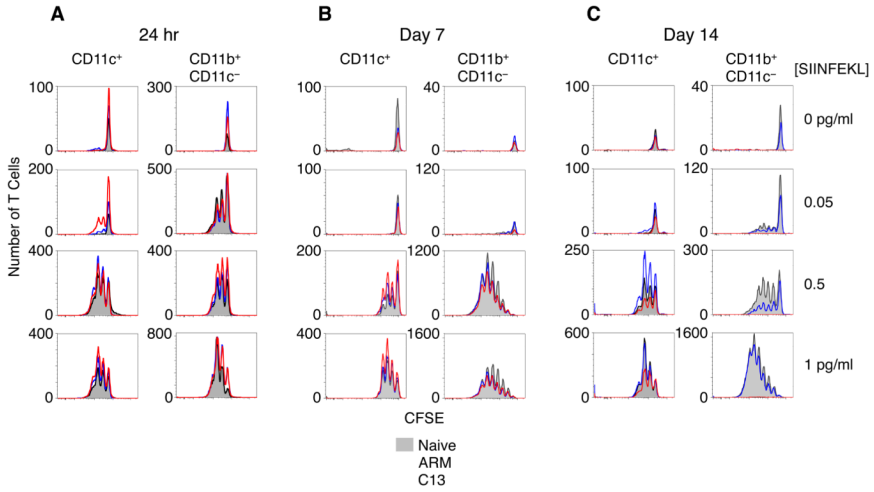

Figure 2. see also Figure S2: CD8$^+$ T Cell stimulatory capacity of APCs from LCMV infected mice

(A) Total proliferating CFSE-labeled OT-I T cells following culture with CD11c$^+$ DC or CD11c$^-$ CD11b$^+$ myeloid cells 24hr p.i. Proliferation was measured by flow cytometry after 3 days of culture with different amounts of SIINFEKL peptide.

(B) Total DC and myeloid cells from day 7 p.i. or day 14 p.i. (C) were bead purified and cultured with purified OVA-specific OT1 T cells as in previous figure.

Data are representative of 3 (A) or 2 (B-C) experiments.

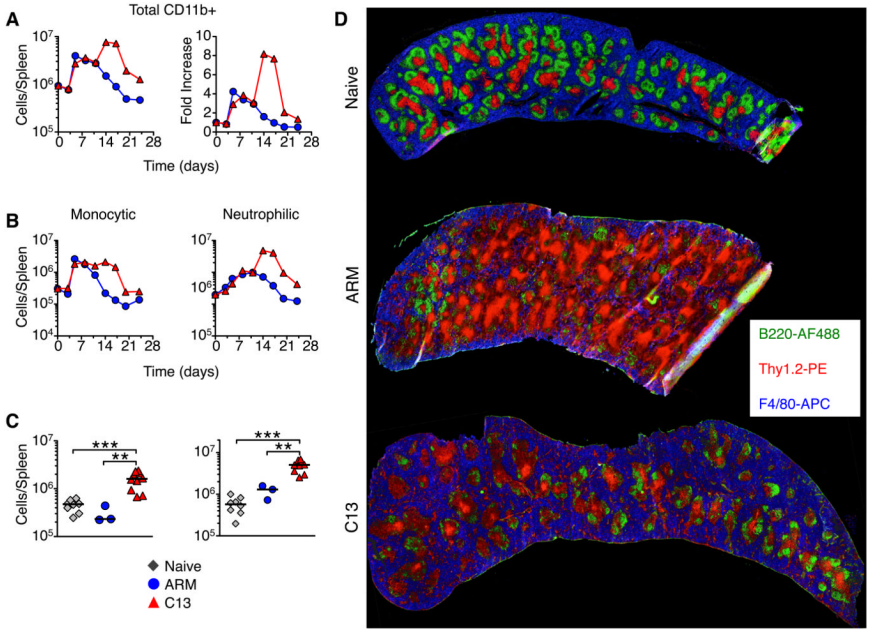

Figure 3. Enhanced and sustained expansion of myeloid cells during chronic LCMV infection

(A) Total splenic $CD11b^+$ myeloid cells during the first 24 days of ARM and C13 infection were enumerated by flow cytometry and the fold increase over naïve levels was determined. Data are representative of 3 experiments and each point represents 3 pooled spleens.

(B) The number of monocytic and neutrophilic cells in the spleen of LCMV infected mice. Data are representative of at least 3 experiments and each point is the mean ± SEM of 3 pooled spleens.

(C) Total number of monocytic and neutrophilic myeloid cells in the spleen of naïve and day 14 LCMV infected mice. Data are individual mice from 4-6 experiments and the bar represents the median. *$p<0.05$, **$p<0.01$, ***$p<0.001$.

(D) Representative histology of mouse spleens from naïve and day 14 LCMV infected mice. $B220^+$ B cells are green, $Thy1.2^+$ T cells are red, and $F4/80^+$ myeloid cells are blue.

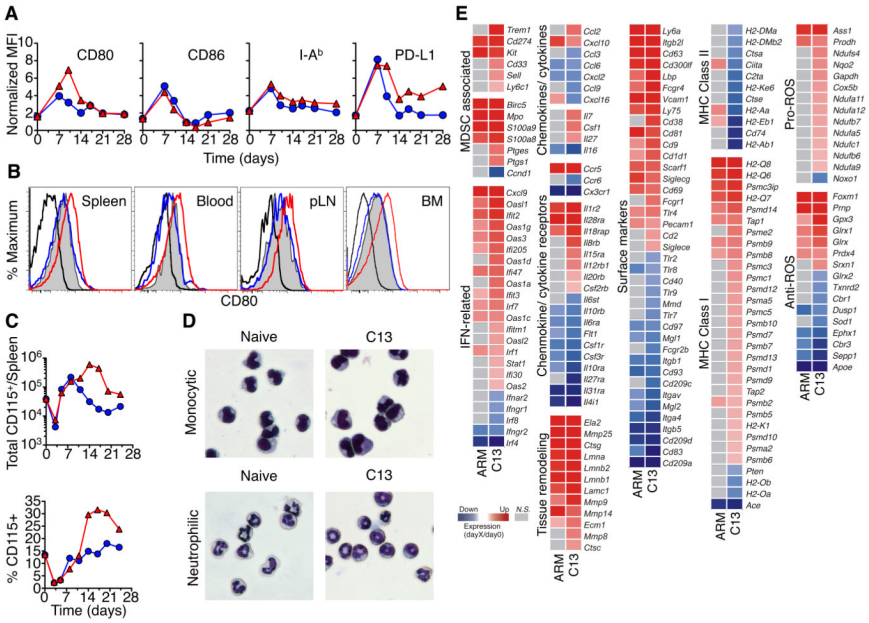

Figure 4. Myeloid cells expanded during chronic infection resemble MDSC

(A) Expression of phenotypic markers on monocytic myeloid cells following LCMV infection.

(B) Expression of CD80 by monocytic cells from multiple organs 14 days p.i.

(C) Kinetics of CD115 expression on total CD11b^{+} cells and myeloid cells. Data are representative of 3 experiments with 3 pooled spleens per group.

(D) Geimsa staining of sorted monocytic and neutrophilic cells from naïve and day 14 C13 infected mice. Data are representative of 3 independent experiments.

(E) Relative expression of genes in monocytic cells from ARM or C13 infected mice compared to naïve mice, as determined by Illumina BeadChips. Genes are ranked by relative expression and represent monocytic cells purified from three independent experiments (mean fold-change).

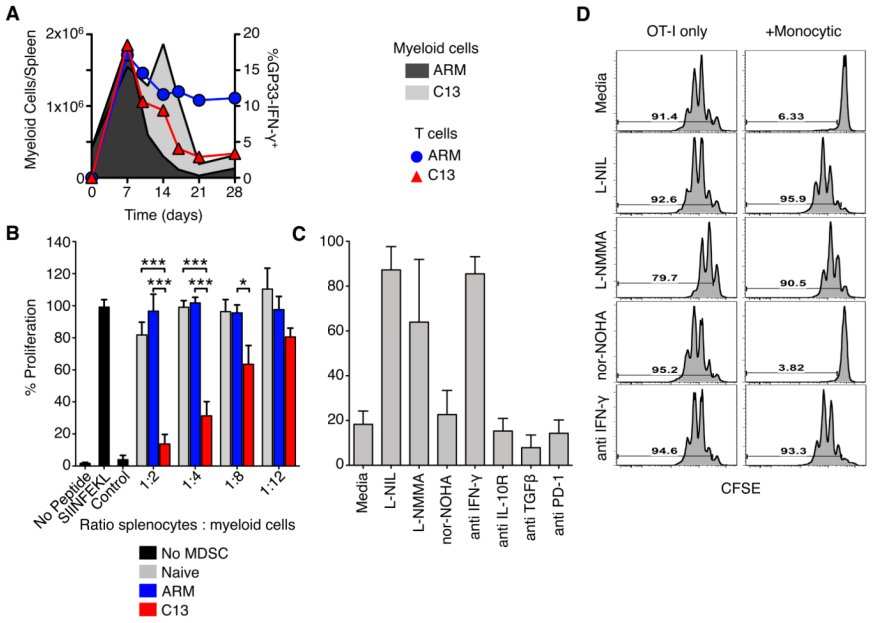

Figure 5. Monocytic cells from C13 infected mice suppress CD8$^+$ T cell proliferation

(A) Total spleen monocytic cells from ARM or C13 infected mice were compared to the frequency of IFN-γ$^+$ GP33-specific CD8$^+$ T cells.

(B) Flow cytometry sorted monocytic cells from day 14 post LCMV infection were cultured with OT-I splenocytes in the indicated ratios. Cultures were stimulated with no peptide, SIINFEKL or vaccinia (B8R) peptide. Proliferation was determined by [^{3} H] Thymidine incorporation.

(C-D) Sorted MDSC from C13 were cultured 1:2 with purified OT-1 T cells and stimulated in the presence of NOS or ARG1 inhibitors or blocking antibodies. Proliferation was measured by CFSE dilution after 3 days of culture.

Percent proliferation was calculated relative to stimulated OT-I splenocytes without added MDSC. Mean ± SEM are performed with 4 experiments performed in triplicate (B) or 3 independent experiments (C-D). *p<0.05, **p<0.01, ***p<0.001.

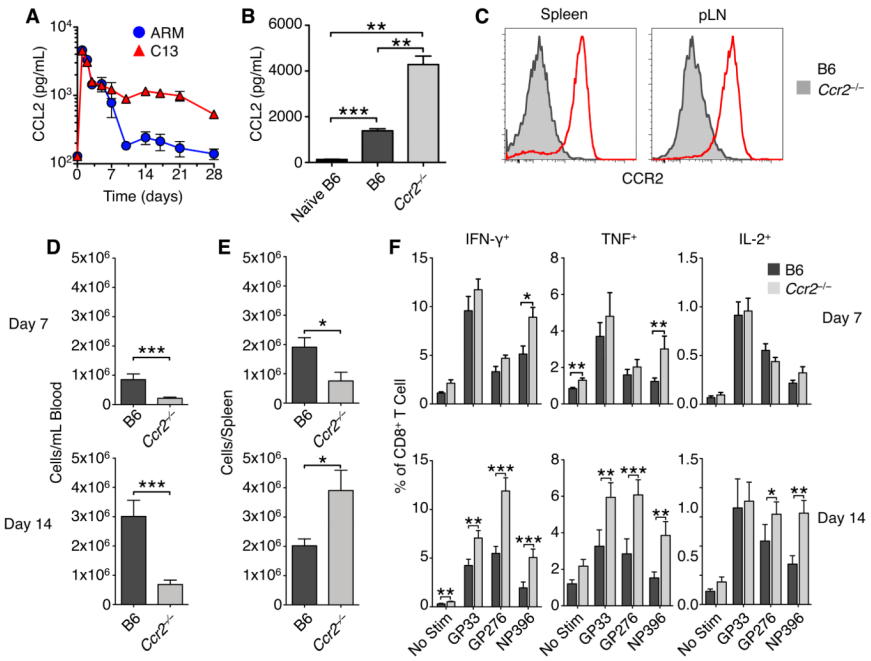

Figure 6. See also Figure S3: CCR2-deficient mice have enhanced T cell responses to C13

(A) Serum concentrations of CCL2 were measured during ARM and C13 infection. Serum cytokine concentrations are presented as mean ± SEM from ≥3 mice per group.

(B) Serum concentrations of CCL2 in WT and *Ccr2*$^{-/-}$ mice day 14 post C13 infection. Serum cytokine concentrations are presented as mean ± SEM from ≥3 mice per group.

(C) Representative flow cytometry CCR2 staining on monocytic cells from WT and *Ccr2*$^{-/-}$ mice day 14 post C13 infection.

(D) Blood and spleen (E) levels of monocytic cells on days 7 and 14 post C13 infection were determined by flow cytometry. Data are represented as mean ± SEM of 3-5 experiments, each with 4-6 mice per group.

(F) Spleen CD8^{+} T cell cytokine production following stimulation with indicated LCMV peptides day 7 and day 14 p.i. Data are represented as mean ± SEM of 3-4 experiments, each with ≥4 mice per group.

*p<0.05, **p<0.01, ***p<0.001.

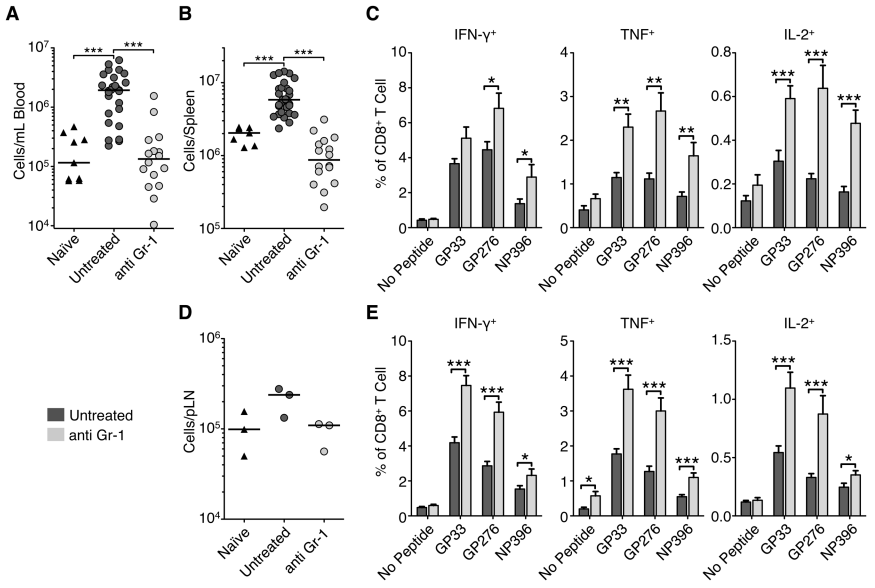

Figure 7. see also Figure S4: Depletion of myeloid cells enhanced LCMV-specific T cell cytokine responses

C13 infected mice received 100μg anti-Gr-1 (RB6-8C5) or isotype control antibody per day starting day 11 p.i. (A) Total myeloid cells ($CD11b^+$ $CD11c^{lo/-}$) in the blood and spleen (B) were measured by flow cytometry on day 14 p.i. Data are individual mice from 3 independent experiments and the bar represents the median.

(C) Frequency of cytokine production in spleen $CD8^+$ T cells following stimulation of splenocytes with indicated LCMV peptides for 5hr and intracellular flow cytometry cytokine staining. Data are represented as mean ± SEM from at least 3 experiments with ≥5 mice per group.

(D) Total myeloid cells in the pooled total pLN. Data are averages of total pLN from 3 mice in 3 independent experiments and the bar represents the median.

(E) Frequency of cytokine production in pLN $CD8^+$ T cells following stimulation with indicated LCMV peptides for 5hr and intracellular flow cytometry cytokine staining. Data are represented as mean ± SEM from 3 experiments with ≥5 mice per group. *p<0.05, **p<0.01, ***p<0.001.